

# Nanofabrication and characterization of a grating-based condenser for uniform illumination with hard X-rays

Jianpeng Liu,<sup>a</sup> Xin Li,<sup>a</sup> Shuo Chen,<sup>a</sup> Sichao Zhang,<sup>a</sup> Shanshan Xie,<sup>a</sup> Chen Xu,<sup>a</sup> Yifang Chen,<sup>a\*</sup> Biao Deng<sup>b</sup> and Chenwen Mao<sup>b</sup>

Received 7 November 2016

Accepted 9 February 2017

Edited by A. F. Craievich, University of São Paulo, Brazil

**Keywords:** condenser; uniform illumination; gratings; nanofabrication; hard X-ray optics.

<sup>a</sup>Nanolithography and Application Research Group, State Key Laboratory of ASIC and System, School of Information Science and Engineering, Fudan University, Shanghai 200433, People's Republic of China, and <sup>b</sup>Shanghai Institute of Applied Physics, Chinese Academy of Sciences, Shanghai 201204, People's Republic of China.

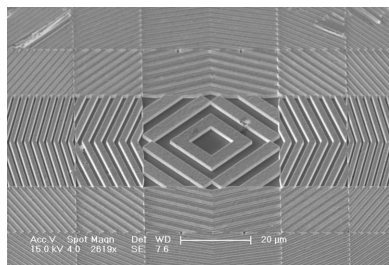
\*Correspondence e-mail: yifangchen@fudan.edu.cn

In the development of full-field transmission X-ray microscopy for basic study in science and technology, a condenser capable of providing intense illumination with high uniformity and stability on tested specimens in order to achieve high-quality images is essential. The latest design of a square-shaped condenser based on diffractive gratings has demonstrated promising uniformity in illumination. This paper describes in more detail the development of such a beam shaper for hard X-rays at 10 keV with regard to its design, manufacture and optical characterization. The effect of the grating profile on the diffracted intensity has been theoretically predicted by numerical simulation using the finite-difference time-domain method. Based on this, the limitations of the grating-based condenser are discussed.

## 1. Introduction

Driven by the critical needs in organic/inorganic chemistry, biology, life science, material science, physics and defect inspection in the semiconductor industry, *etc.*, full-field transmission X-ray microscopy (TXM) is becoming a powerful technique in nano-scale detection (Myneni *et al.*, 1999), owing to its unique capability in non-destructive three-dimensional imaging of specimens in real time with high resolution (Chen *et al.*, 2011). One of the key components in TXM is the condenser, which de-magnifies the X-ray beam from the light source to form a shaped illumination in a certain area on the specimen to be tested (Rudati *et al.*, 2011). To achieve high-quality imaging, it is primarily required to provide an intense, stable and uniform illumination in an area on the specimen under test. High stability of illumination can be readily achieved by situating the whole transmission X-ray microscope on a heavy marble platform to eliminate any mechanical vibrations at all frequencies. Also, the environmental temperature is controlled within  $\pm 1^\circ\text{C}$  to minimize any thermal disturbances. Damage to golden condensers by X-ray radiation at 8–10 eV has not been observed so far in our laboratory. Therefore, the major concern for a condenser is the uniformity of its illumination on specimens.

The typical size of the required illumination area is in the range of a few tens of micrometres, depending on the particular geometry of the setup. Earlier methods for lighting specimens were to use optics such as Fresnel zone plates (Anderson *et al.*, 2000), tapered capillaries (Yin, 2006), mirrors (Naulleau *et al.*, 2003) and combinations of these devices



(Niemann *et al.*, 2003). Unfortunately, these optics focus the beam into a spot smaller than the field of view (FOV) of the microscope, resulting in non-uniform illumination. Large-area illumination with significant improvement in uniformity was achieved by Vogt *et al.* (2006), who cleverly divided a condenser zone plate into many sectors as single pitched gratings. The overall illumination of the lighted area is the superposition from all the sectors, leading to good uniformity in a circular-shaped area (the same as the sector) but with clear tails on the edge. In matching the FOV with CCD detectors, which are usually square-shaped, a significantly improved design of such a beam shaper based on gratings was first proposed by Jefimovs *et al.* (2008). Uniform illumination without the unwanted tails in both soft (500 eV and 720 eV) and hard (8 keV) X-ray wavelengths was successful.

Following this idea, this paper describes, in more detail, the development of such a square condenser with regard to its design, fabrication and characterization for hard X-rays at 10 keV. At the end of the paper, the contradiction between the illumination uniformity and the intensity of the grating-based condenser is discussed, based on our numerical simulation of the effect of the grating profile on the distribution of diffracted intensity.

## 2. Design of the square condenser

The design of the square condenser is based on the diffraction principle of X-rays by gratings with certain pitch which defines the project direction, as schematically illustrated in Fig. 1. The overall area of the condenser should be close to that of the beam to minimize loss of energy. The condenser is divided into sub-fields of the same area ( $a \times a$ ) as the illuminated one on the specimen. Each sub-field is a linear grating with a specific pitch. The orientation of the grating lines and the pitch should be carefully calculated to ensure that the diffracted light is projected onto the same illuminated region on the specimen. The first diffraction order of the gratings is used to light the focal plane, *i.e.* the specimen, of the condenser. Thus, the total illumination on the tested specimen is the superposition of the diffracted light from all sub-fields, resulting in uniform lighting (Jefimovs *et al.*, 2008).

Based on the principle described above, it is not difficult to calculate the line orientation and the pitch of the  $(i,j)$ th grating in the condenser as

$$r_{i,j} = a(i^2 + j^2)^{1/2}. \quad (1)$$

For the distance of the  $(i,j)$ th grating to the condenser centre, where  $a$  is the edge length of the sub-field,

$$p_{i,j} = \lambda \left[ (D/r_{i,j})^2 + 1 \right]^{1/2}, \quad (2)$$

which is the pitch of the  $(i,j)$ th grating, where  $\lambda$  is the wavelength and  $D$  is the focal length. Obviously, the grating line

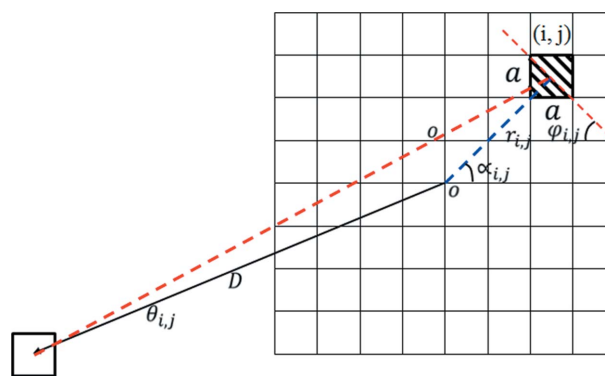


**Figure 1** Schematic diagram showing the illumination principle by the square condenser composed of sub-fields with specific gratings. The symbols in the diagram are defined in the text. Each sub-field should be the same as the illuminated area on the specimen.

orientation in the  $(i,j)$ th field should be  $\tan \phi_{i,j} = ij$  and the diffraction angle  $\theta_{i,j}$  follows  $\tan \theta_{i,j} = j/i$ . Due to the fourfold symmetry, only one-quarter of the condenser should be calculated. Fig. 2 shows the actual design of the condenser layout following equations (1)–(2). In this work, the overall area of the condenser is  $400 \mu\text{m} \times 400 \mu\text{m}$  and the FOV is  $20 \mu\text{m} \times 20 \mu\text{m}$ . The pitch of the outermost grating is 400 nm.

## 3. Nanofabrication of the square condensers

Nanofabrication was carried out by the standard process for gold zone plates (Liu *et al.*, 2015) on a 100 nm-thick  $\text{SiN}_x$  membrane. State-of-the-art electron beam lithography was first adopted to define the grating patterns in the condenser in a 2.5  $\mu\text{m}$ -thick PMMA as the template for the subsequent deposition of gold. A Monte Carlo simulation was conducted using the simulators of *Layout-BEAMER/TRACER/LAB* supplied by GenISys Ltd to calculate the optimized spatial distribution of injected charge in the electron beam exposure in such thick PMMA (Liu *et al.*, 2015), trying to minimize

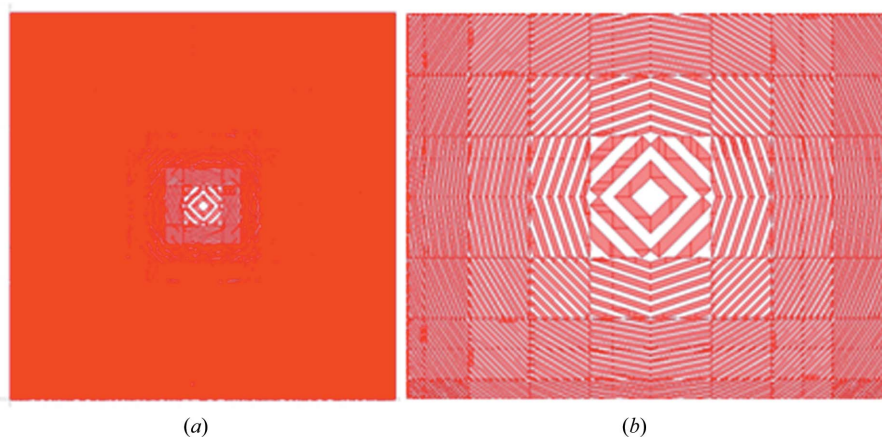


**Figure 2** Designed layout of the square condenser composed of gratings. (a) Overall condenser, (b) central part.

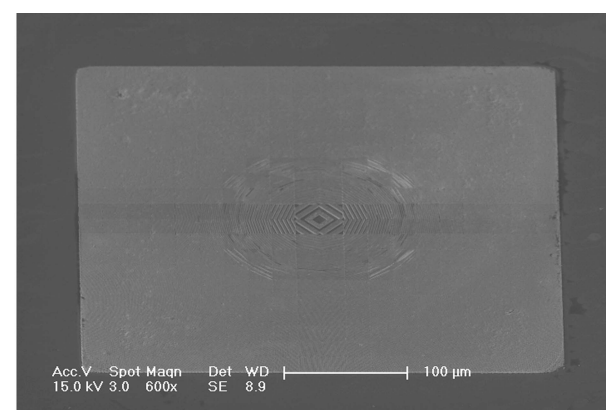
trench-width spreading caused by the forward scattering of incident electrons. Electron beam exposure was performed using an 8 nm beam in a Jeol 6300FS system at 100 keV. The optimized dose was figured out in the range 1600–1700  $\mu\text{C cm}^{-2}$ , which is a reasonably large window. Electroplating was carried out in a cyanide-based electrolyte, driven by a constant current source delivered by Keithley Ltd. A lift-off process consisting of soaking the condenser in warm

acetone for about 20 min successfully removed the unwanted PMMA.

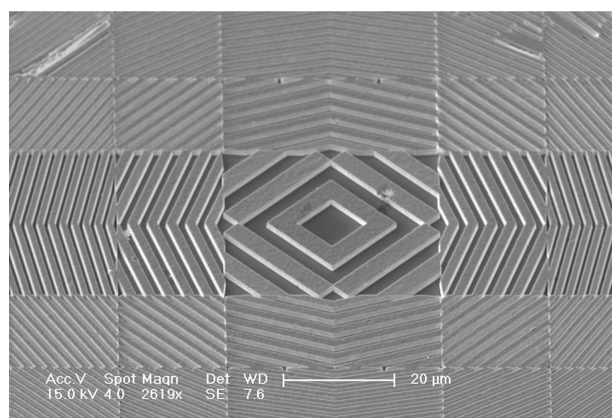
Fig. 3 presents the fabricated square condenser in gold, standing on a 100 nm-thick  $\text{SiN}_x$  membrane. The height of the gratings in the condenser is 2.4  $\mu\text{m}$ , which is essential to shape the hard X-rays at 10 keV in this work.

#### 4. Optical characterization and discussion

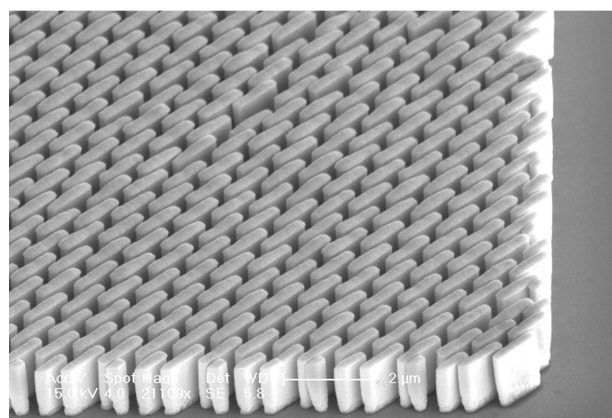
The illumination quality through the fabricated square condenser was then characterized by a 10 keV beam at the BL15U beamline of Shanghai Synchrotron Radiation Facility. The real measurement set-up is shown in Fig. 4(a), and a schematic diagram in Fig. 4(b) describes the optical path in the measurement. To protect the detector from being damaged by the zero-order light, a thick gold beam-stop was arranged in the central part of the condenser. The diameter of the beam-stop was 40  $\mu\text{m}$  and the thickness was 80  $\mu\text{m}$ . The diameter of the order-sorting aperture (OSA) was 30  $\mu\text{m}$ . The incident X-rays passed through the outskirts of the condenser and condensed onto a scintilla in the visible microscope.



(a)



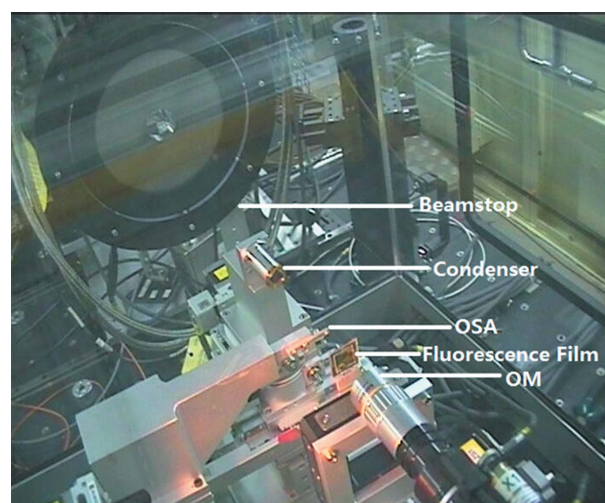
(b)



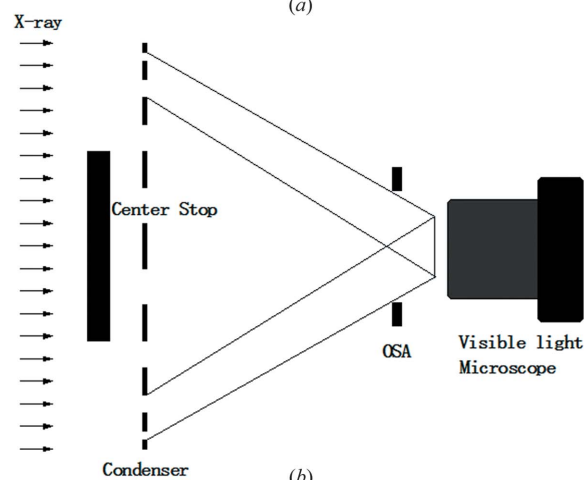
(c)

**Figure 3**

Micrographs obtained by the scanning electron microscope, Sigama HD delivered by ZEISS Ltd, for the fabricated square condensers. (a) Overall view of the condenser at low magnification, (b) central part and (c) one of the corners showing the 12:1 aspect ratio of the gold grating lines.



(a)



(b)

**Figure 4**

Optical measurement setup at the BL15U beamline of Shanghai Synchrotron Radiation Facility. (a) Photograph of the setup, and (b) schematic of the optical path in the measurement.

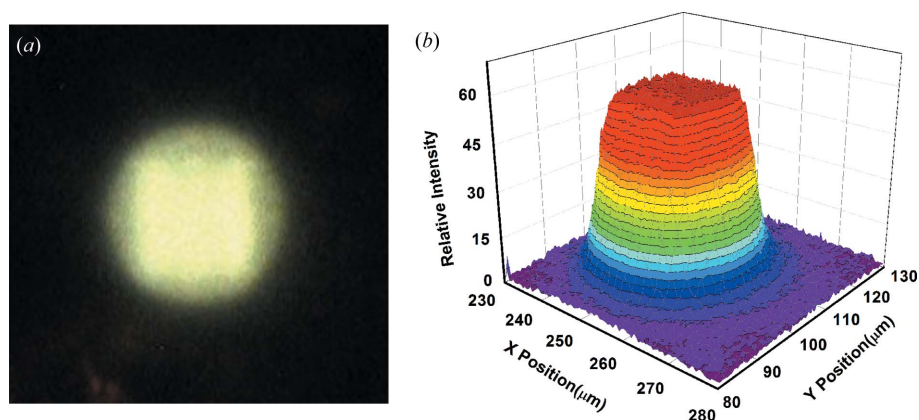


**Figure 5**  
Optical measurement results at the beamline. (a) Image of the fabricated condenser on the focal plane by the visible microscope with X-rays at 10 keV. (b) Measured intensity distribution in 3D at the focal plane.

Fig. 5(a) shows an image of the condenser obtained using a high-resolution X-ray detector placed in its focal plane. A well defined square shape in the lighting area can be observed. From the two-dimensional brightness of the image the distribution of the relative intensity is obtained and presented in Fig. 5(b). A flat top of around  $20\ \mu\text{m} \times 20\ \mu\text{m}$  can be clearly observed, which agrees with the designed sub-field size in Fig. 2 as the illumination area. Fig. 6 shows the intensity changing

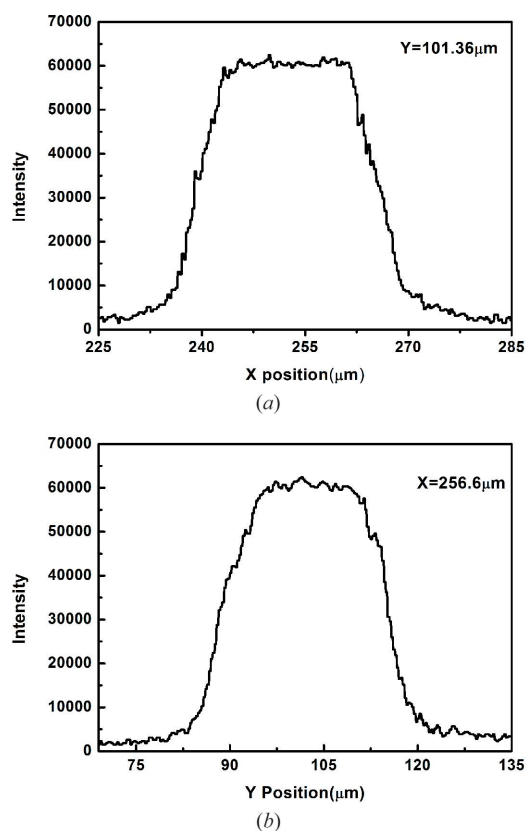


**Figure 6**  
Measured intensity along the x-axis (a) and the y-axis (b). The flat top of the illuminated area shows uniform illumination quality by the fabricated square condenser.

along the x-axis and the y-axis through the centre of the illumination image. The standard deviation of the illumination intensity within the illuminated region on the focal plane is 1.1%, indicating that an outstanding uniformity is achieved by the square condenser in this work.

However, the indistinct edges of the illumination outside the  $20\ \mu\text{m} \times 20\ \mu\text{m}$  uniform area can also be seen as shown in Fig. 6(a). There may be two factors responsible for this undesired illumination. One is the low monochromaticity of the beam and the extended source could cause the indistinct edge of the illumination. In this work, the monochromator is made from

single-crystal Si with (111) surface, whose monochromaticity is  $\Delta\lambda/\lambda = 1.5 \times 10^{-4}$  at 10 keV. The beam is from a vertical slit of width  $50\ \mu\text{m}$ . The other possible cause is the random scattering of the light in the YAG scintillator that could result in leakage of the light, especially when its thickness is comparable with the dimensions of the illuminated area in this work. Since the thickness of the beam-stop in our experiment is as thick as  $80\ \mu\text{m}$ , the possibility of transmission through the stop should be ruled out. Therefore, to eliminate the unwanted illumination outside the designed area, all the above-mentioned factors should be carefully considered.

High-quality imaging by a TXM requires not only high uniformity in the illumination as described above but also high intensity on the tested specimen. Despite the great success in achieving high uniformity by the grating-based condenser, as demonstrated by Jefimovs *et al.* (2008) as well as in this paper, the limitation in diffraction efficiency of this brand of beam shapers still remains a concern. As is well known, the diffraction efficiency of gold gratings is theoretically limited to  $4/\pi^2$  ( $\sim 40\%$ ) for rectangular-shaped phase gratings (Rayleigh, 1888; Wood, 1898). To enhance the efficiency beyond the limit of the rectangular gratings, non-rectangular profiles such as parabolic or step-shape of the grating should be considered (Tatchyn *et al.*, 1984). Unfortunately, it is found in this work that non-rectangular gratings are likely to disturb the spatial distribution of the diffracted intensity, causing non-uniform illumination on the testing specimens. The effect of the grating profile on the illumination uniformity is theoretically simulated in this work by finite difference time domain (FDTD) methods. As shown in Fig. 7, the transmitted intensity near gratings with three different profiles is compared. Non-symmetry distribution of the intensity is observed in both non-rectangular gratings, which may damage the uniformity in the illumination. It also implies that the defects in gratings may destroy the uniform illumination. Therefore, although the grating-based condenser is able to provide highly uniform illumination, it might suffer from limited intensity due to the low diffraction efficiency. The trade-off between high uniformity by rectangle-shaped gratings and high diffraction effi-

ciency by modifying the binary grating profile needs to be balanced to meet the requirements for both high symmetric distribution in the intensity and high diffraction efficiency.

It is also necessary to mention that the grating-based condenser in this work is designed for a specific wavelength, *i.e.* a certain X-ray energy only. In some applications when energy scanning is required, such a condenser is not applicable. This may be another limitation of the condenser used in this work.

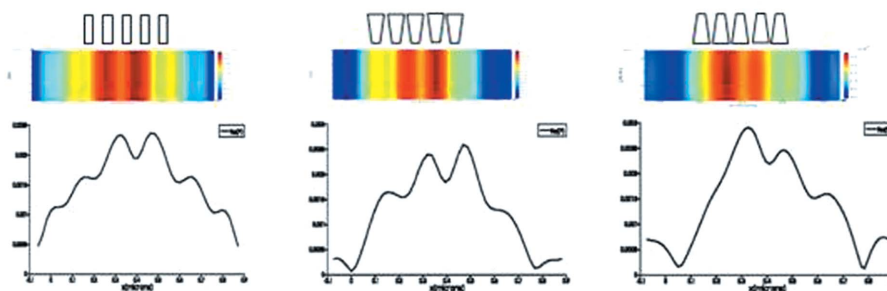


**Figure 7** Simulation results for the effect of the grating profile on the diffracted intensity distribution. Three different grating profiles corresponding to rectangular (a), up-side down trapezium (b) and trapezium (c) are compared. The intensity distributions calculated by the FDTD method show that the illumination can be significantly altered by the grating profile.

## 5. Conclusion

This paper describes, in explicit detail, the design, fabrication and optical characterization of a grating-based condenser for uniform illumination in hard X-ray TXM, based on the diffraction principle by gratings as proposed in the literature. A condenser with  $400\ \mu\text{m} \times 400\ \mu\text{m}$  view field was designed and fabricated by a conventional zone plate process. Optical characterization demonstrates that the fabricated condenser is able to condense the 10 keV X-rays from the source to the specimen in a  $20\ \mu\text{m} \times 20\ \mu\text{m}$  area with a 1.1% uniformity. The performance limitation in illumination intensity for such a square condenser is tackled by a FDTD simulator. The contradiction between uniform illumination and high intensity may be solved by optimizing the grating profile so that such a square condenser can be successfully applied for hard X-ray optics in full-field TXM.

## Acknowledgements

The research described in this paper was financially supported by Professor Yifang Chen's Pump Priming Fund under the Thousand Talents Program.

## References

- Anderson, E. H., Olynick, D. L., Harteneck, B., Veklerov, E., Denbeaux, G., Chao, W., Lucero, A., Johnson, L. & Attwood, D. (2000). *J. Vac. Sci. Technol. B*, **18**, 2970–2975.
- Chen, T. Y., Chen, Y. T., Wang, C. L., Kempson, I. M., Lee, W. K., Chu, Y. S., Hwu, Y. & Margaritondo, G. (2011). *Opt. Express*, **19**, 19919–19924.
- Jefimovs, K., Vila-Comamala, J., Stampanoni, M., Kaulich, B. & David, C. (2008). *J. Synchrotron Rad.* **15**, 106–108.
- Liu, J. P., Shao, J., Zhang, S., Ma, Y., Taksatorn, N., Mao, C., Chen, Y., Deng, B. & Xiao, T. (2015). *Appl. Opt.* **54**, 9630–9636.
- Myneni, S. C. B., Brown, J. T., Martinez, G. A. & Meyer-Ilse, W. (1999). *Science*, **286**, 1335–1337.
- Naulleau, P. P., Goldberg, K. A., Batson, P., Bokor, J., Denham, P. & Rekawa, S. (2003). *Appl. Opt.* **42**, 820–826.
- Niemann, B., Guttman, P., Rehbein, S. & Knöchel, C. (2003). *J. Phys. IV (Paris)*, **104**, 273–276.
- Rayleigh, L. (1888). *Sci. Papers*, **III**, 47–187.
- Rudati, J., Irwin, J., Tkachuk, A., Andrews, J. C., Pianetta, P. & Feser, M. (2011). *AIP Conf. Proc.* **1365**, 136–139.
- Tatchyn, R., Csonka, P. L. & Lindau, I. (1984). *J. Opt. Soc. Am. B*, **1**, 806–811.
- Vogt, U., Lindblom, M., Charalambous, P., Kaulich, B. & Wilhein, T. (2006). *Opt. Lett.* **31**, 1465–1467.
- Wood, R. W. (1898). *Philos. Mag. Ser. 5* **45**, 511–522.
- Yin, G. C. (2006). *Appl. Phys. Lett.* **89**, 221122.